

Radial Velocity and Metallicity of the Globular Cluster IC4499 Obtained with AAOmega ^{*}

Warren J. Hankey¹ and Andrew A. Cole¹

¹*School of Mathematics & Physics, University of Tasmania, Private Bag 37, Hobart, TAS 7001, Australia; warren.hankey@utas.edu.au*

1 November 2018

ABSTRACT

We present radial velocity and metallicity measurements for the far-southern Galactic globular cluster IC 4499. We selected several hundred target red giant stars in and around the cluster from the 2MASS point source catalog, and obtained spectra at the near-infrared calcium triplet using the AAOmega spectrograph. Observations of giants in globular clusters M4, M22, and M68 were taken to provide radial velocity and metallicity comparison objects. Based on velocity data we conclude that 43 of our targets are cluster members, by far the largest sample of IC 4499 giants spectroscopically studied. We determine the mean heliocentric radial velocity of the cluster to be 31.5 ± 0.4 km/s, and find the most likely central velocity dispersion to be 2.5 ± 0.5 km/s. This leads to a dynamical mass estimate for the cluster of $93 \pm 37 \times 10^3 M_{\odot}$. We are sensitive to cluster rotation down to an amplitude of ≈ 1 km/s, but no evidence for cluster rotation is seen. The cluster metallicity is found to be $[\text{Fe}/\text{H}] = -1.52 \pm 0.12$ on the Carretta-Gratton scale; this is in agreement with some earlier estimates but carries significantly higher precision. The radial velocity of the cluster, previously highly uncertain, is consistent with membership in the Monoceros tidal stream as proposed by Peñarrubia and co-workers, but also with a halo origin. The horizontal branch morphology of the cluster is slightly redder than average for its metallicity, but it is likely not unusually young compared to other clusters of the halo. The new constraints on the cluster kinematics and metallicity may give insight into its extremely high specific frequency of RR Lyrae stars.

Key words: stars: radial velocities – stars: abundances – stars: late-type – globular clusters: individual (IC 4499)

1 INTRODUCTION

IC 4499 is a sparsely populated globular cluster in a crowded galactic field near the south celestial pole. It was discovered in 1900 by D. Stewart (Pickering, 1908) and has been comparatively understudied, probably as its extreme southern declination presents an observational challenge to mid-latitude observers. Several photometric studies of IC 4499 have been undertaken to study the horizontal branch (HB) morphology, produce colour-magnitude diagrams (CMDs) and make distance and metallicity estimates, but no detailed spectroscopic metallicity or radial velocity data have been published to date.

The globular cluster catalogue of Harris (1996) gives a distance of 18.9 kpc, which puts it 15.7 kpc from the Galac-

tic centre and 6.6 kpc below the plane of the galaxy, making it an outer halo cluster. From the vantage point of Earth, it is seen through the outer parts of the Galactic bulge ($\ell = 307.35^{\circ}$, $b = -20.47^{\circ}$), resulting in a relatively high reddening. This reddening has been estimated as high as $E(B-V) \approx 0.35$ (Fourcade et al., 1974), but more recent work suggests smaller values of 0.15–0.25 (Sarajedini, 1993; Storm, 2004; Walker & Nemeč, 1996; Ferraro et al., 1995). The uncertainty in reddening has likely propagated through into differences in conclusions about the metallicity, distance, and age of IC 4499.

Low-resolution spectroscopic radial velocities and metallicities have been obtained for three RR Lyrae stars only (Smith & Perkins, 1982). They obtain a metallicity of $[\text{Fe}/\text{H}] = -1.33 \pm 0.3$ from the strength of the singly-ionised Ca II K line using the ΔS method (Smith, 1984). On the scale of Zinn & West (1984, ZW84) this becomes $[\text{Fe}/\text{H}] = -1.5 \pm 0.3$. Fusi Pecci et al. (1995) noted a discrepancy between photometric metallicity estimates, which tend to be

^{*} Based on observations made with the Anglo-Australian Telescope operated at Siding Spring Observatory by the Anglo-Australian Observatory.

around $[\text{Fe}/\text{H}] \approx -1.75$ (Ferraro et al., 1995) and the generally higher spectroscopic estimates. More recent unpublished work by R. Cannon (1992) is quoted by Sarajedini (1993) and Walker & Nemeč (1996) as yielding $[\text{Fe}/\text{H}] = -1.65$ on the ZW84 scale, based on the near-infrared Ca II triplet lines of four red giants. Smith & Perkins (1982) also published radial velocities for their three RR Lyrae stars, -60, +10 and -101 km/s, all with an error of ± 50 km/s.

IC 4499 is noteworthy in having an extremely high specific frequency of RR Lyrae variables; its value of $S_{RR} = 113.4^1$ is second only to the smaller Fornax 1 globular cluster (Mackey & Gilmore, 2003) and the tiny outer halo cluster Pal 13 (Harris, 1996). About 100 RR Lyrae stars have been identified and represent $\approx 68\%$ of the total HB population (Sarajedini, 1993). Most of the RR Lyr have $P \leq 0.6$ d, making it an Oosterhoff Type I (OoI) cluster (Clement et al., 2001; Walker & Nemeč, 1996). Metallicity may be an important factor in determining the Oosterhoff classification of a cluster, as most OoI clusters tend to be more metal-rich than $[\text{Fe}/\text{H}] = -1.8$ on the ZW84 scale, while Oosterhoff Type II clusters more metal-poor (Sandage, 1993). It is thought that shorter-period RR Lyrae stars have not evolved off of the zero-age horizontal branch (ZAHB), while the longer-period variables are evolving through the RR Lyr instability strip on the way to the asymptotic giant branch. The measurement of accurate cluster parameters therefore has the potential to shed light on the evolutionary pathways of horizontal branch stars (e.g., Clement & Rowe, 2000; Pritzl et al., 2000).

IC 4499 has been proposed as a “young” globular cluster with an age 2-4 Gyr younger than clusters with similar metallicity (Ferraro et al., 1995), where age is established by differential magnitude and colour comparisons with the main-sequence turnoff (TO). The method compares magnitude difference between the HB and TO, and the colour difference between the red giant branch (RGB) and TO. In clusters of similar metallicity, the magnitude difference increases and the colour difference decreases with increasing age. Ferraro et al. (1995) adopt a value of $[\text{Fe}/\text{H}] = -1.8$ on the ZW84 scale in their work, and find that IC 4499 is essentially coeval with Arp 2 and NGC 5897. However, this matter is not settled, as the similarly-derived compilation of 55 globular cluster ages by Salaris & Weiss (2002) finds an age of 12.1 ± 1.4 Gyr for IC 4499, not significantly younger than the average of metal-poor clusters. While the latter study assumed the cluster was 0.3 dex more metal-rich than Ferraro et al. (1995) did, they arrived at a similar conclusion about the cluster coevality with Arp 2 and NGC 5897. A careful consideration of the cluster metallicity must be made in order to help resolve this discrepancy.

Fusi Pecci et al. (1995) noted that IC 4499 lies near a great circle around the Galaxy that passes through other possibly “young” globulars, including Pal 12 and Rup 106. This suggestion is a forerunner of the modern studies of halo substructure based on searching for tidal streams and RGB overdensities. In the past decade there has been a rapidly growing awareness of substructures in the Galactic halo (e.g., Morrison et al., 2000; Yanny, 2000;

Vivas, 2001; Newberg et al., 2002). Apart from the tidal stream of the disrupting Sagittarius dwarf spheroidal, one of the strongest structures detected in photometric surveys is the Galactic Anticentre Stellar Structure, which is also known as the Monoceros tidal stream or ring (e.g., Newberg et al., 2002; Ibata et al., 2003). The Monoceros stream may be associated with the tidal disruption of a dwarf galaxy close to the plane of the Milky Way, possibly the Canis Major dwarf (e.g., Helmi et al., 2003; Martin et al., 2005); it is also possible that the Monoceros stream is a dynamical structure intrinsic to the thick disk of the Milky Way (e.g., Piatti & Clariá, 2008; Younger et al., 2008). Several Milky Way star clusters have been suggested as members of the Monoceros stream (Martin et al., 2004; Frinchaboy et al., 2004; Peñarrubia et al., 2005; Piatti & Clariá, 2008; Warren & Cole, 2009, and numerous references therein), and this could have strong impacts on studies of the statistics of the Milky Way globular cluster population if a number of clusters are found to have extragalactic origins.

No observational study of the Monoceros stream covers the neighbourhood of IC 4499. However, a set of numerical models of the stream, developed under the hypothesis that it is the remnant of a disrupting dwarf galaxy, have been proposed by Peñarrubia et al. (2005). In one of their best models, stellar debris stripped from a progenitor dwarf at $\ell = 245^\circ$, $b = -18^\circ$ encircles the Milky Way within $\pm 30^\circ$ of the Galactic plane, crossing the location of IC 4499 after nearly a complete wrap. Peñarrubia et al. (2005) suggested that IC 4499, along with several other clusters, could be candidate members of the stream on the basis of their position and the predicted radial velocities in their models. The radial velocity of IC 4499 has not yet been determined accurately enough to check for consistency with this type of model.

Following the methodology of Warren & Cole (2009), we have undertaken a spectroscopic study of IC 4499’s red giants in order to obtain radial velocity and metallicity measurements for a large sample of cluster members; the aim is to shed light on questions of its relative age and possible membership in a stellar stream. We employ the relationship between CaII triplet line strengths and $[\text{Fe}/\text{H}]$ to obtain metallicity estimates for individual giants. The near-infrared CaII triplet, resulting from absorption by the $3^2\text{D}-4^2\text{P}$ transition, is a strong feature of late-type giant stars (Armandroff & Zinn, 1988). The equivalent width of the lines increases monotonically with metallicity, regardless of age, for stars older than 1 Gyr (e.g., Garcia-Vargas et al., 1998).

Spectroscopy of the near-infrared calcium triplet in spectral type K giants has become an accepted tool for assessing the metallicity of stellar populations (Armandroff & Da Costa, 1991), being calibrated against Galactic globular clusters (Rutledge et al., 1997). Originally used in studies of old, simple stellar populations, the technique has been shown to apply to non-globular cluster stars, including open clusters and composite populations (e.g. Cole et al., 2004; Grocholski et al., 2006; Battaglia et al., 2008, and references therein).

The line strength has a strong dependence on surface gravity and a milder temperature dependence (Armandroff & Zinn, 1988; Garcia-Vargas et al., 1998),

¹ $S_{RR} \equiv N_{RR}10^{0.4(7.5+M_V)}$ for a cluster of absolute magnitude M_V with N_{RR} variables.

which is removed using the empirical relationship between gravity, temperature, and luminosity for red giant stars. (Rutledge et al., 1997) showed that using the stellar apparent magnitude with respect to the cluster horizontal branch is a robust approach to this procedure. Because of the availability of JHK_S photometry and astrometry in the 2MASS catalog, we adopt the K-band as our reference magnitude, following Warren & Cole (2009). Their relationship between $K - K_{HB}$, $[Fe/H]$, and Ca II equivalent width is confirmed by our observations of IC 4499 and three other clusters.

We discuss our approach, observations, reductions, and analysis in the next section. Because using K magnitudes to correct for surface gravity is relatively novel compared to V or I, we rederive the relation between K_s magnitude above the horizontal branch and CaII line strength. Using three well-studied clusters as a calibration sample, we present new abundance and radial velocity measurements for IC 4499 in §3. We examine our data for signs of cluster rotation, and rule out rotation velocities in IC 4499 of 1 km/s or more. In §4 we discuss the implications of our results, including the contention that IC 4499 is younger than the bulk of halo globulars (Ferraro et al., 1995; Fusi Pecci et al., 1995), and the possibility that IC 4499 belongs to the Monoceros stellar stream (Peñarrubia et al., 2005).

2 METHODOLOGY

2.1 Observations

Observations were carried out on 28 May 2008 at the 3.9m Anglo-Australian Telescope at Siding Spring Observatory. The seeing was 1.4". The AAOmega fibre-fed multi-object spectrograph (MOS) allows for up to 392 simultaneous spectra to be obtained, across a two degree field of view (Sharp et al., 2006). The 1700D grating was used, which gives a spectral resolution of about 10,000 $[\lambda/\Delta\lambda]$, varying slightly across the field. This grating spectrum is in the the near-infrared with usable $\lambda\lambda$ 8450 to 8700 Å, which includes the ionised calcium triplet lines at 8662, 8542 and 8498 Å. This feature is among the strongest lines in K-type giants (Armandroff & Da Costa, 1986), which is the dominant spectral type for red giants at low-metallicity.

Targets were chosen from the 2MASS point source catalogue (PSC), which has a positional accuracy of about 100 mas (Skrutskie, 2006); this accuracy is crucial to the success of the observations because of the necessity to accurately place the 2.0" fibres on the targets. The selection was based on 2MASS J and K photometry with K between 10.5 and 15.0. Because of the slope of the RGB, the color selection had a slope as well, although quite steep. The red limit was set by $K > 27.0 - 15(J - K)$, and the blue limit was set by $K < 22.5 - 15(J - K)$. The selection region is shown on the CMD in Figure 1. The highest MOS fibre allocation priority was given to stars within the cluster half-light radius and in the upper 2.25 mag of the RGB.

The half-light and tidal radii of IC 4499 are 1.5' and 12.35', respectively (Harris, 1996). Fibres were preferentially allocated to the centre of the 2° field. Once the cluster centre was sampled as densely as possible with fibres, the spare fibres were allocated to stars outside the cluster centre in the same colour and magnitude range. This should allow for a

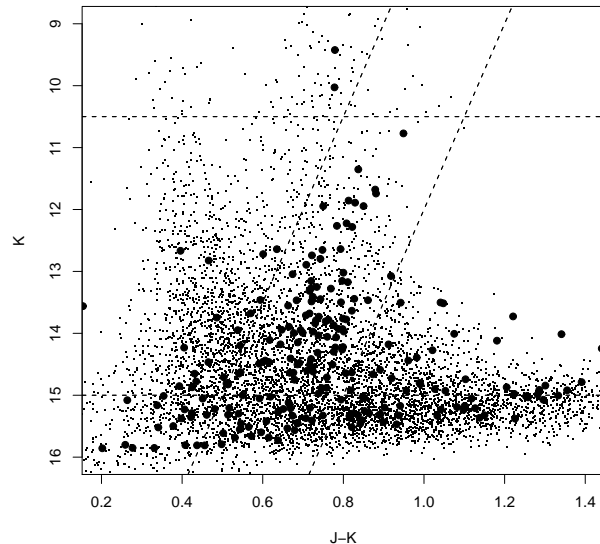


Figure 1. Selection of RGB stars from 2MASS PSC within 1° of the centre of IC 4499. Objects within 5' of the cluster centre are plotted with large symbols to highlight the cluster RGB relative to the field. Our spectroscopic sample is selected from candidates within the parallelogram containing the cluster RGB.

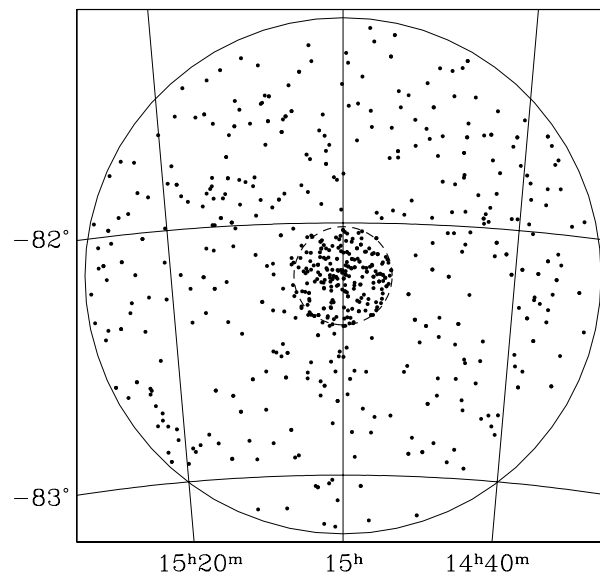


Figure 2. Observed targets in a 2° field around IC 4499. The tidal radius is shown by the dashed line; the fibre allocation was strongly weighted to select targets within this radius.

very precise characterisation of the radial velocity distribution of the field stars, to assist with membership decisions. Because of the density of the cluster, not all stars could be observed in a single setup. We observed two different fibre configurations with the same central position in order to maximise the yield of members. In total 569 individual stars

were observed with signal to noise ≥ 15 per pixel in a two degree field around IC 4499; the targets are mapped in Figure 2. The fields were integrated over several exposures to mitigate systematic errors and cosmic ray contamination. The total exposure time for each IC 4499 setup was 3600 sec.

Three well-studied clusters were chosen as comparison objects. These were picked to yield stars of similar spectral type and metallicity to use as radial velocity templates in our cross-correlation, and to confirm that we could reproduce the relationship between K magnitude and CaT equivalent width across a range of metallicities. We used M68 (NGC 4590), M4 (NGC 6121), and M22 (NGC 6656) as our comparison objects; their positions, relevant properties, and observing details are listed in Table 1. For the calibration clusters, RGB stars were chosen from 2MASS J and K photometry in the regions of the selected clusters. (J–K, J) CMDs were created for square-degree areas centred on each cluster, and targets were selected from the cluster RGB locus down to and including the HB. We tried to sample as wide a range of magnitude as possible in each cluster in order to accurately model the influence of surface gravity on the CaT equivalent widths. In general, there are relatively few bright RGB stars, and the brightest, coolest stars are often contaminated by titanium oxide bands in the spectral region of interest, so sampling the bright end of the RGB while respecting the restrictions on minimum fibre spacing was a challenge. In most cases, the cluster RGB sequences are not clearly distinct from the surrounding field, and the samples were cleaned according to radial velocity and position relative to the cluster centre. The individual spectra of each target were coadded after extraction and dispersion correction.

Calibration exposures including arc lamp and screen flats were taken between each pair of science exposures in order to allow for dispersion correction and flatfielding. Sky subtraction was achieved using 20–25 dedicated sky fibres per setup, except in the case of M68, where an offset sky exposure was taken.

2.2 Data Reduction and Analysis

Data reduction was accomplished using the standard AAOmega reduction software *2dfdr drcontrol*. The reduction software automatically corrects for CCD bias with blank frames and an overscan bias region. Individual fibre images were traced on the CCD and then dispersion corrected, wavelength-calibrated spectra were extracted using standard procedures from arc lamp exposures and flat fields. The M68 sky subtraction was achieved by stacking and averaging the offset sky spectra. The spectra from separate exposures of the same target were combined using the IRAF *imcombine* tool. The spectra were normalised by fitting a fifth order polynomial model to the continuum with the IRAF *oned-spec.continuum* task. Residual cosmic rays in the combined exposures were removed by applying simple clipping. Given the large sample size, visual inspection of each spectrum was impractical, so dead fibres, non-stellar objects, and targets with poor signal-to-noise due to fibre-centring errors were rejected automatically. Figure 3 shows a typical normalised spectrum. The spectral resolution achieved was 0.9 \AA , with

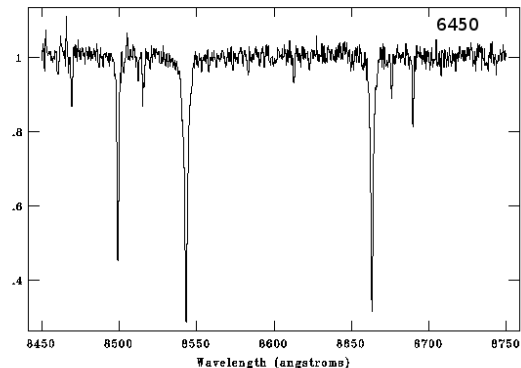


Figure 3. Typical spectrum of IC 4499 member RGB star showing the Ca II triplet and many weaker metal lines. Star I.D. 6450 in Table 3

a typical signal-to-noise ratio in the continuum of 50:1 per pixel.

2.3 Radial Velocities

After the data reduction process a total of 36 stars from the calibration clusters with velocities from the literature were chosen to be used as radial velocity templates. Published references provided online electronic data for M22 and M4 (Peterson & Cudworth, 1994) (Peterson et al., 1995), which were matched with our observations using the ESO SKYCAT software tool. In the case of M68 we used the published finding charts from Harris (1975) to identify the reference stars. The chart positions were visually compared with maps made from the 2MASS catalogue to match the velocities quoted by Harris to our targets.

Of the 36 available reference stars, 19 had excellent signal to noise ratio, no cosmic rays and good sky subtraction residuals. Originally only these 19 reference spectra were employed, but it subsequently proved statistically advantageous to use all available reference spectra to reduce the standard error in the mean of the 36 cross correlations. Fifteen stars from M4, twelve from M22 and nine from M68 provided a representative sample of the reference clusters. The IRAF task *fxcor* was used to calculate the velocities of the IC 4499 stars by cross correlation with the set of reference spectra (Tonry & Davis, 1979). The normalised continuum level was subtracted and a Gaussian fitted to the cross correlation to establish the velocity.

The velocity of our target stars was derived from a weighted average of cross-correlation velocities from the individual template stars. The average was constructed after automatic rejection of templates that gave large velocity errors, using a Grubb test. The velocities based on each remaining template were then averaged, with weighting based on the cross-correlation errors.

Stars were defined as members of the cluster using three parameters. Firstly by distance from the cluster centre, stars within the tidal radius (catalogued by Harris, 1996) were selected. Secondly, stars were selected around velocity overdensities. In the case of the calibration clusters these velocity distributions were located as expected according to previ-

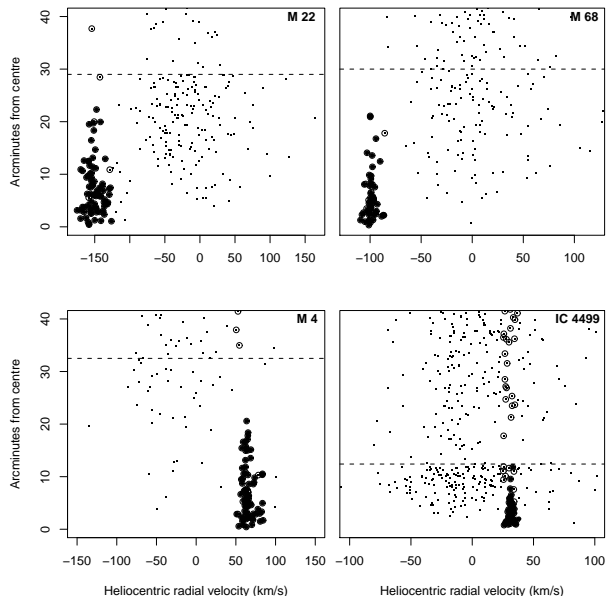


Figure 4. Velocities and distances from the cluster centres. The tidal radii are shown by dashed lines. Stars within the tidal radius that survived a radial velocity and metallicity cleaning are shown as solid circles. Open circles mark stars with a radial velocity that matches the cluster but fall outside the tidal radius, or have Ca II equivalent widths much different from the cluster members.

ous studies. Stars that appeared to be normally distributed about these mean values were selected as probable members. Figure 4 shows the low velocity-dispersion distributions between the cluster centre and the tidal radius from which stars were selected. Some contamination of the sample from field stars with similar velocities is expected, although this is small for the calibration clusters. Stars were finally selected based on the measured equivalent widths of the three Ca II triplet lines as described in the next section. Apertures were rejected in cases of low S/N, contamination by cosmic rays or other artifacts. These features resulted in odd equivalent width measurements.

The range of velocities in the disk, outer bulge, and halo towards IC 4499 is quite large, and there are several field stars projected within the tidal radius. All velocities have been translated to the heliocentric reference frame within *fccor*, based on the time and date of the observations. The mean cluster velocities are given in Table 2. The velocities are in good agreement with literature references for M22 and M68, but our mean is 5.2 km/sec (4.7σ) away for M4; the origin of this difference is unknown. The mean heliocentric radial velocity of IC 4499 is $31.5 \pm 0.4 \text{ km/sec}$. As seen in Figure 5, this is sufficiently different from the bulk of the field star velocities to allow the cluster to be defined, but there is some overlap.

2.4 Cluster Rotation

Lane et al. (2009) find a rotational signature in M22 and a suggestion of one in M68. They also find rotation in M4 (Lane et al., 2010). While we have a much smaller sample of stars, we can also look for such a signature. We employ

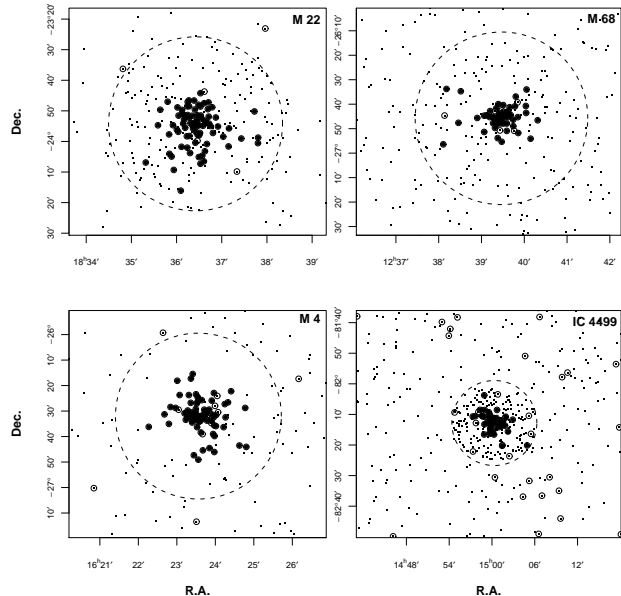


Figure 5. Cluster member map. Solid circles are cluster members. Open circles with similar velocities were rejected for lying outside the tidal radius, (dashed line), as metallicity outliers, or for contaminated spectra.

Lane et al. (2009)’s method to look for signatures of rotation in M4, M22 and M68 as a check, and then in IC 4499. The position angle of the cluster rotation axis is not known a priori, so a search of parameter space is made to see if the cluster radial velocities are consistent with rotation around an arbitrary axis. For a given trial position angle we divide the cluster in half along a line 90° away and compare the mean velocity in each half of the cluster. We step around the cluster in position angle increments of 22.5° . The asymmetric sky distributions of the samples, (see Figure 5), alias with bin sizes and angular location adding to uncertainty. The differences in mean radial velocity between the cluster halves at each position angle are plotted in Figure 6.

We agree with Lane et al. (2009) on the rotation amplitude in M22: we find a line of sight rotational value of $1.8 \pm 0.7 \text{ km/s}$ and the axis of rotation approximately North-South, at $114^\circ \pm 18^\circ$, where they found $1.5 \pm 0.4 \text{ km/s}$, approximately North-South. M4 shows amplitude $2.1 \pm 0.4 \text{ km/s}$ and axis roughly North East-South West at $30^\circ \pm 12^\circ$, about double the result of Lane et al. (2010) who obtain $0.9 \pm 0.1 \text{ km/s}$ at an angle of 70° as do Peterson et al. (1995). There is no evidence for cluster rotation in the data for M68 and IC 4499 above the error level of 0.4 km/s . Our M22 and M4 data show that we are sensitive to rotation velocities down to at least $\approx 1 \text{ km/s}$, and this must therefore be a strict upper limit to the rotation of IC 4499. No correction for rotational velocity in IC 4499 is necessary when calculating velocity dispersion in the following section.

2.5 Virial Mass and Mass to Light Ratio

In order to estimate the cluster mass we need to assume a model for the cluster gravitational potential and use the central velocity dispersion, σ_0 , and the virial theorem. Fol-

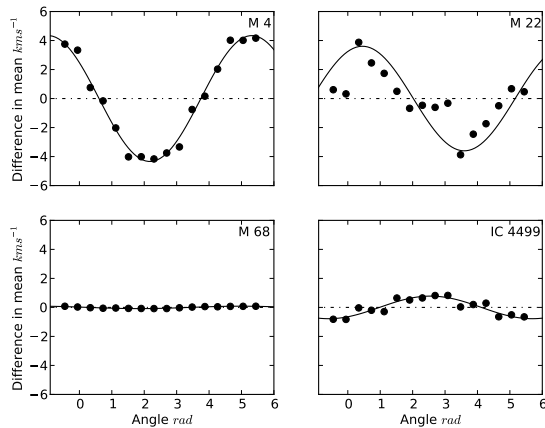


Figure 6. Results of cluster rotation searches shows the difference in mean radial velocity between two halves of the cluster divided by a line orthogonal with the listed position angle. Position angle is defined anticlockwise from East ($PA=0$) through North ($PA=\frac{\pi}{2}$) around the centre of light of the cluster. The best-fitting sine curve is shown.

lowing Lane et al. (2010), a Plummer-type spherical model for the cluster mass distribution is used, (Plummer, 1911). Assuming isotropic velocities one can calculate a mass using the central velocity dispersion σ_0 , where,

$$M = \frac{64\sigma_0^2 R}{3\pi\mathcal{G}}$$

where R is the half-light, or scale, radius and \mathcal{G} is the gravitational constant.

To estimate σ_0 , Lane et al. (2010) first bin the velocities by radius, then use a Markov Chain Monte Carlo (MCMC) technique to estimate dispersions within the bins and subsequently fit a Plummer model. We have taken a different course, preferring not to bin the velocities, but choosing instead to fit the Plummer model to the individual data points. We assume that the individual observations are Normally distributed

$$v_i \sim N(\mu, \sigma^2(r))$$

where the line of sight velocity dispersion $\sigma(r)$ is determined by a Plummer model

$$\sigma^2(r) = \frac{\sigma_0^2}{\sqrt{1 + (r/R)^2}}.$$

Here σ_0 , the central velocity dispersion, is the main parameter of interest, R the half light radius and μ the systemic mean cluster velocity. Assumptions are made about the initial distributions of parameters, an improper uniform prior for μ , and weakly informative Normal priors for R and σ_0 . We then fit the model by MCMC using a Metropolis within Gibbs algorithm (Gilks et al., 1998). There were 26×10^3 samples drawn, with the first 6×10^3 discarded as ‘burn-in’, an initial period where the Markov Chain explores parameter space.

The median value of the distribution of σ_0 samples is 2.5 ± 0.5 km/s. The median is used as an estimator as the distribution is skewed toward higher values, because the model has a lower bound for central velocity dispersion at zero,

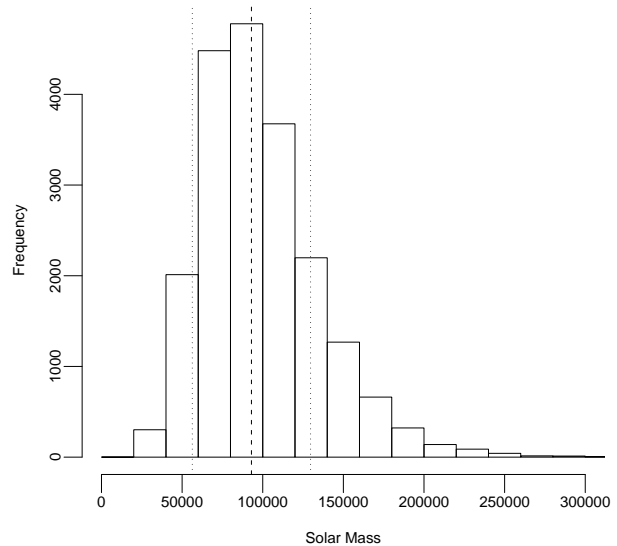


Figure 7. Distribution of Markov Chain Monte Carlo simulations of mass, based on a central velocity dispersion model. Standard deviation $37 \times 10^3 M_\odot$ is shown around the median value, $93 \times 10^3 M_\odot$.

but no upper bound. Velocity dispersion has not been constrained to zero at the tidal radius as in a King model (King, 1966). The mean value is thus slightly higher at 2.6 km/s. The value of μ , the cluster mean systemic velocity from MCMC simulation is 31.5 km/s and agrees with the classical sample mean estimator, the sum of velocities divided by the number of samples. The value of the half light radius from simulation is $102 \pm 18''$ and agrees within error with the starting reference value of $107 \pm 19''$ (Trager et al., 1993).

The distribution of cluster mass, a function of the velocity dispersion samples from MCMC simulation, is shown in Figure 7. The median mass is $93 \pm 37 \times 10^3 M_\odot$ where the error is 1σ . McLaughlin & van der Marel (2005) also estimate a mass for IC 4499 using a power law model, as well as King and Wilson models, fitted to the light distribution of the cluster. They obtain mass estimates of $125 - 138 \times 10^3 M_\odot$ for IC 4499 and central velocity dispersions of 2.88 – 2.96 km/s. This spectroscopic study finds a lower value but agrees with the photometry-based results within errors. For an absolute magnitude $M_V = -7.33$, we estimate a mass to light ratio of $1.3 \pm 0.5 M/L_V$ in solar units. Our lower mass gives a smaller value than McLaughlin & van der Marel (2005) who estimate 1.874. This M/L_V ratio is similar to other globulars and indicates that there is not a significant dark matter component to the cluster.

2.6 Equivalent Widths and Metallicities

The cluster samples are each assumed to represent a single stellar population. The sample does not include any stars above the RGB tip, where lower surface gravity results in the line width being more sensitive to metallicity (Garcia-Vargas et al., 1998), or low temperature M stars where line width responds more to effective temperature re-

sulting in lower values, and TiO bands confuse the interpretation.

Low signal-to-noise spectra in which one or more of the Ca II triplet lines were badly distorted were rejected. As a diagnostic we compared the ratios of each line with respect to the others. A line with too large or small a value with respect to the others indicates a problem with the data or the line fitting results. Spectra with odd line ratios were rejected from further analysis. In Figure 8 the ratios are plotted for an IC 4499 cluster sample to identify outliers.

A wavelength range is chosen in the spectrum that encompasses the line feature and a representative portion of the normalised continuum. The line and continuum bandpasses are taken as defined in Armandroff & Da Costa (1991). The sum of a Gaussian and a Lorentzian, a Penny function, is fitted to the line profiles using the same FORTRAN code as Cole et al. (2004), which is a modified version of the code of Armandroff & Da Costa (1986), to give an equivalent width for each line. The Penny function has been shown to be a better approximation for high metallicity, high resolution spectra (Warren & Cole, 2009). Model atmospheres of late-type giants indicate the wings are more sensitive to metallicity than other parameters such as surface gravity and effective temperature (Smith & Drake, 1990).

The equivalent widths of the three triplet lines are summed to give the CaII index. Some authors sum the two strongest lines for low signal to noise data or low resolution spectra (Rutledge et al., 1997). Here, having a high signal to noise ratio, the sum of three lines is taken to give the full equivalent width ΣW . Results for ΣW in the sample stars in IC 4499 are shown in Table 3.

Next a reduced equivalent width W' is derived in which the linear dependence on the magnitude height on the RGB is taken into account. This *magnitude* parameter represents the effects of the effective temperature and stellar surface gravity on the line strengths (Armandroff & Da Costa, 1991). Because red giants lie along a narrow sequence in the luminosity (surface gravity) vs. temperature plane, T_{eff} and $\log g$ are correlated with each other and their influence on ΣW can be calibrated out using a single observable. Colour and absolute magnitude have both been used in the past to create the index W' , but the most robust method in the presence of distance and reddening uncertainties is to use an expression relating the magnitude of the target star to the mean magnitude of the horizontal branch (or red clump) of its parent population (Rutledge et al., 1997).

Owing to the availability and homogeneity of 2MASS near-infrared magnitudes, we adopt the procedure of Warren & Cole (2009) and use the K-band magnitude, $K - K_{HB}$ to derive W' . Warren & Cole (2009) defined $W' = \Sigma W + 0.45(K - K_{HB})$; because it is uncommon to use the K band in this procedure, the slope is not as well-determined as that in V or I, so we rederive the relationship as a consistency check.

The mean value of the RR Lyrae variable magnitudes is used to define the horizontal branch K-magnitude, 12.21 for M22, 11.13 for M4 and 15.97 for IC 4499. K-magnitudes for RR Lyrae variables in IC4499 are found in Storm (2004) and define the magnitude of the horizontal branch. There are K-magnitudes for a few RR Lyrae stars in M22 (Kaluzny & Thompson, 2001), and several for M4 (Liu & Janes, 1990). Many more M4 variables are

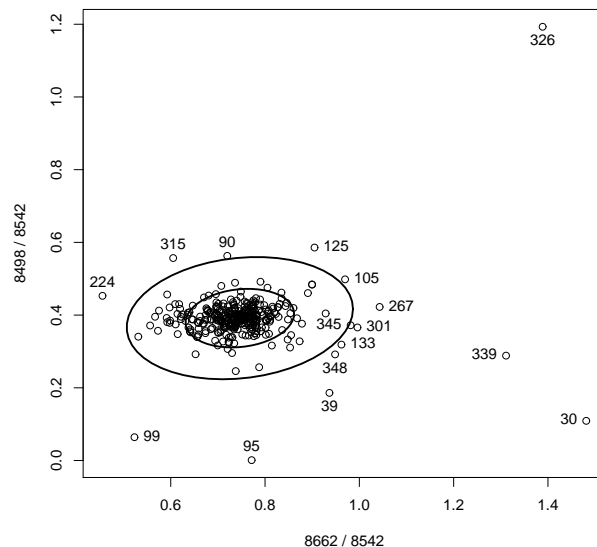


Figure 8. Plot of line width ratios of apertures in an IC 4499 field, with 50% and 95% confidence contour. Outlying points were considered statistically unlikely, and rejected aperture numbers are shown .

listed in Longmore et al. (1990). RR Lyrae variables in M22 and M4 were identified from those catalogued in Clement et al. (2001) and these were astrometrically correlated with 2MASS objects to obtain K magnitudes. M68 horizontal branch K-magnitude of 14.4 is referenced from Ferraro et al. (2000) and Dall’Ora et al. (2006). For each cluster K_{HB} is taken to be constant and each star in the 2MASS PSC has a unique $K - K_{HB}$.

We plot the relative magnitude $K - K_{HB}$ against the equivalent width ΣW in Figure 9. The slopes of the lines β_K range from $0.29 \leq \beta_K \leq 0.65$, with a mean value of $0.47 \pm 0.08 \text{ \AA/mag}$. This agrees well with the value of $\beta_K = 0.48 \pm 0.01$ found by Warren & Cole (2009), who have 22 clusters, open and globular, in their sample. There is no strong reason to suspect variation in β for a globular cluster-only sample (Rutledge et al., 1997), so we adopt the better-determined value $\beta_K = 0.48 \pm 0.01$ from Warren & Cole (2009). The *reduced* equivalent width W' , is the intercept of this linear model. W' should be a constant for each cluster that only depends on metallicity. Fits to our four clusters and the literature slope are shown in Figure 9 and the values of W' listed in Table 2.

W' is related linearly to $[\text{Fe}/\text{H}]$ on the Carretta & Gratton (1997) scale; we follow Warren & Cole (2009) who arrived at the following relation for transforming to metallicity:

$$[\text{Fe}/\text{H}] = (-2.738 \pm 0.063) + (0.330 \pm 0.009)W'$$

The values of $[\text{Fe}/\text{H}]$ derived from this relationship are given in Table 2. They agree with the literature values to better than 1σ , as expected. As emphasised by Cole et al. (2004); Warren & Cole (2009), these values are specific to the Carretta & Gratton (1997) metallicity scale. Recalibration to ZW84, the scale of Kraft & Ivans (2003), or any other

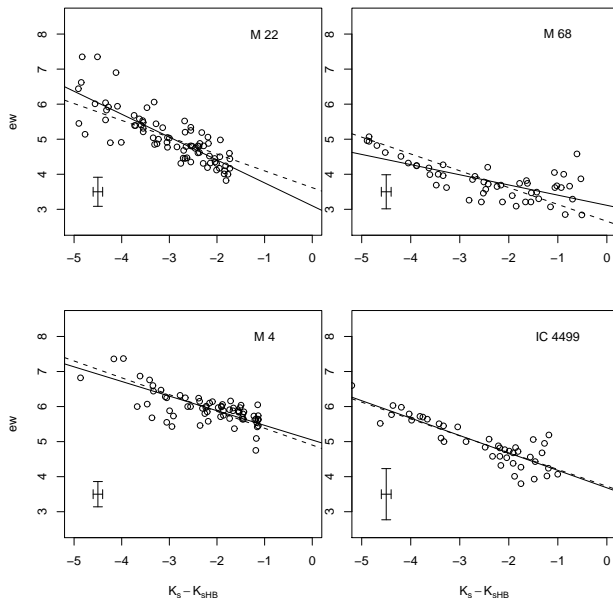


Figure 9. $K_s - K_{s,HB}$ vs. ΣW for our clusters. The dashed line shows the average slope from Warren & Cole (2009), and the solid lines give the best-fit slope for each individual cluster based on our data. Typical errorbars are shown in the lower left of each panel. The intercept of the relation defines the *reduced* equivalent width W' for each cluster.

metallicity scale of choice may be achieved using the W' values, which give the correct relative metallicity ranking of the clusters no matter the specific $W' - [\text{Fe}/\text{H}]$ conversion adopted.

3 THE VELOCITY AND METALLICITY OF IC 4499

Identifications, positions, velocities and equivalent widths for individual IC 4499 stars are given in Table 3. The metallicity of IC 4499 is very similar to the mean metallicity of M22, $[\text{Fe}/\text{H}] = -1.52 \pm 0.12$, and the radial velocity is $v_r = 31.5 \pm 0.4$ km/s. This is the first published spectroscopic metallicity measurement for the cluster based on more than just a few stars. Previous estimates for the radial velocity varied widely and are difficult to properly assess.

Smith & Perkins (1982) derived a spectroscopic metallicity of $[\text{Fe}/\text{H}] = -1.33 \pm 0.3$ from three RR Lyrae variables in IC 4499. ZW84 revise this figure by recalibrating to the scale of Frogel et al. (1983) and quote $[\text{Fe}/\text{H}] = -1.5 \pm 0.3$. Ferraro et al. (1995) found this value to be too high, and adopted -1.75 based on the CMD morphology, primarily HB type and RGB colour. Later studies of the RR Lyrae population (e.g., Walker & Nemeč, 1996) found no inconsistencies with this value, and cite an unpublished study by R. Cannon finding $[\text{Fe}/\text{H}] = -1.65$ in support. Our value of $[\text{Fe}/\text{H}] = -1.52 \pm 0.12$ on the Carretta & Gratton (1997) scale translates to $[\text{Fe}/\text{H}] = -1.74 \pm 0.10$ on the ZW scale. M22, a cluster with very similar W' , has $[\text{Fe}/\text{H}] = -1.75$ according to Carretta & Gratton (1997), and $[\text{Fe}/\text{H}] = -1.9$ on the scale of Kraft & Ivans (2003), according to Da Costa et al. (2009). The latter paper also finds strong

evidence for an internal spread of metallicities in M22 of up to 0.5 dex, so more detailed comparison to M22 may only serve to confuse the picture. However, we can confirm that the RR Lyrae-based result from Smith & Perkins (1982) for IC 4499 is too metal-rich, and the CMD results are robust.

The radial velocity measurement is relatively unexceptional, as a wide range of velocities are expected towards the 4th quadrant of the Galaxy. The Besançon model Galaxy (Robin et al., 2003) shows that radial velocities toward IC 4499 have a broad maximum around -15 km/s, with $\text{FWHM} \approx 60$ km/s. If only the stars with $[\text{Fe}/\text{H}] \leq -1$ are considered, the mean radial velocity is expected to be ≈ 25 km/s, with a very broad distribution: the FWHM of metal-weak stars in this direction is ≈ 110 km/s, and with tails reaching to $-150 \lesssim v_r \lesssim +350$ km/s. IC 4499 thus lies near the peak of the expected radial velocity distribution of halo stars in this direction. We are in disagreement with the average velocity of 3 RR Lyrae stars, -50 km/s, reported by Smith & Perkins (1982). Other velocity measurements are scarce; Peñarrubia et al. (2005) place IC 4499 in their Fig. 11 with $v_r = 0$, without attribution. Similarly, Fusi Pecci et al. (1995) give the cluster a galactocentric radial velocity $v_{r,GC} \approx -130$ km/s, also without citing a source. The Fusi Pecci et al. (1995) value is not far from the measured value of v_r if we account for the solar motion; we find $v_{r,GC} = -140$ km/s.

3.1 Is IC 4499 Unusual?

IC 4499 has an exceptionally high frequency of RR Lyrae stars (e.g., Walker & Nemeč, 1996, and references therein), and has been proposed to be 2–4 Gyr younger than the average of metal-poor clusters (Ferraro et al., 1995). It is also a candidate to belong to halo substructures (Fusi Pecci et al., 1995), including the possibility of membership in the Monoceros tidal stream if that structure is due to the dissolution of a dwarf galaxy in the tidal field of the Milky Way (Peñarrubia et al., 2005). These suggestions hint towards the idea that the HB morphology can be connected to some combination of age and/or detailed elemental abundance ratios (e.g., differences in $[\alpha/\text{Fe}]$). A further clue may be in the fact that the cluster is of Oosterhoff type I, that is, the RR Lyrae stars have periods $\lesssim 0.6$ d.

It is well-known that the Oosterhoff type of a cluster is related to its metallicity (e.g., Walker & Nemeč, 1996), but the relation is not a straightforward one. In general, the period of the variation increases with decreasing metallicity, but several clusters have been found that appear to break the rules. NGC 6388 and NGC 6441 (Pritzl et al., 2000), are metal-rich clusters displaying properties of both Oosterhoff types.

Sandage (1993) noted that there are very few variables in clusters with $-1.7 \leq [\text{Fe}/\text{H}] \leq -1.9$ on the ZW84 scale, and that the few known RR Lyrae stars present have longer than expected periods. However, he assumed $[\text{Fe}/\text{H}] = -1.5$ for IC 4499, where it should have a $[\text{Fe}/\text{H}] = -1.75$ on the ZW84 scale. Clusters of similar metallicity indeed tend to have much smaller specific frequencies of RR Lyrae stars (e.g., M22 has $S_{RR} = 7.2$, Harris, 1996). This is likely because most of the HB stars at this metallicity begin their lifetimes well to the blue of the RR Lyrae instability strip (Lee et al., 1990). The extremely high specific frequency of

RR Lyrae stars at the metallicity of IC 4499 suggests a larger than average stellar mass at the zero-age horizontal branch (ZAHB). As noted by Walker & Nemeč (1996), this could be indicative of a younger than average age for the cluster, or it could suggest a smaller-than-average amount of mass-loss along the cluster RGB; Sandage (1993) already suggested that a smaller-than-average *dispersion* in mass-loss was necessary to reproduce the colour extent of IC 4499's HB. IC 4499's lower-than-average central density compared to clusters like M3 may be related to its RGB mass-loss behaviour. It is also possible that variations in the detailed elemental abundances, such as $[\text{O}/\text{Fe}]$, play a role in determining the HB morphology.

We find M22 to have similar average metallicity to IC 4499; it has few RR Lyrae stars, a blue HB, and a higher central density, and is an OoII type cluster. This makes the 2 clusters something like a classical “second parameter” pair like M3 and M2, both with $[\text{Fe}/\text{H}] \approx -1.6$ on the CG97 scale. Lee & Carney (1999) have proposed that there is an age difference between the two clusters of ≈ 2 Gyr, in accordance with the arguments in, e.g., Lee (1992). This is similar to the argument in Ferraro et al. (1995) that IC 4499 is $\approx 2\text{--}4$ Gyr younger than similar-metallicity halo clusters. However the picture is complicated here because of the existence of a significant range of abundances in M22 (Da Costa et al., 2009). IC 4499 appears to have a slightly unusual Lee (1989) HB type for its metallicity, but a younger than average age cannot definitely be stated to be the cause. According to the models in Lee (1992), an age difference of $\lesssim 1$ Gyr compared to M3 would be required to account for the relatively red HB morphology; the difference would be smaller if smaller-than-average mass-loss is adopted. Comparing to the HB types of other candidate “young” globulars, IC 4499 is likely to be significantly older than Rup 106, and some of the outer halo clusters like Pal 4 and Eridanus. This complicates the suggestion in Fusi Pecci et al. (1995) for a common origin shared between Rup 106 and IC 4499.

Salaris & Weiss (2002) found that IC 4499 was nearly coeval with other intermediate-metallicity clusters. However, they assumed an incorrect metallicity, $[\text{Fe}/\text{H}] = -1.26$ (CG97), and the comparison should be redone using the more accurate value $[\text{Fe}/\text{H}] = -1.52 \pm 0.12$. Salaris & Weiss (2002) conclude that all clusters with $[\text{Fe}/\text{H}] \leq -1.2$ appear to be coeval within errors, at an age of ≈ 12 Gyr. Forbes & Bridges (2010) argue that there is a break in the age-metallicity relation for galactic globular clusters at $[\text{Fe}/\text{H}] \approx -1.5$. While there exists a class of old clusters at higher metallicity, there appears to be a group of young clusters with metallicities above the break point which they identify as accreted “young halo” clusters. Like Salaris & Weiss (2002), Forbes & Bridges (2010) find those classified as “old halo” are roughly coeval at ≈ 12.8 Gyr. If a reanalysis of the cluster CMD is made, using the new spectroscopic metallicity, that still suggests an age difference relative to the bulk of halo globulars, then the conclusion of Salaris & Weiss (2002) would be challenged and it would suggest that IC 4499 belongs to the “young” group of Forbes & Bridges (2010) clusters.

Carollo et al. (2007) hypothesise that halo objects are divided into two main classes, with the outer halo having lower metallicity and odd orbits suggesting accretion from low-mass dwarf galaxies, while the inner halo is higher

metallicity and galactic in origin. IC 4499 has a smaller galactocentric distance than typical outer halo clusters, but its location where models predict an extension of the Monoceros tidal stream (Peñarrubia et al., 2005) may strengthen the idea that it has an extragalactic origin. The evidence for membership in the Monoceros stream to date has been based solely on its position within a modeled extension of the stream. At the location of IC 4499, these models predict a radial velocity that ranges between $-60 \text{ km/s} \leq v_r \lesssim 100 \text{ km/s}$, which has nearly complete overlap with the standard Galactic halo model for this sightline (Robin et al., 2003). An interesting feature of the Peñarrubia et al. (2005) model is that as in Fusi Pecci et al. (1995), Rup 106 and IC 4499 are suggested to be members of a single dynamically-related feature, but in the Monoceros stream model Rup 106 belongs to the trailing side of the tidal stream, while IC 4499 is a member of the leading stream. Both clusters have drifted a large distance from their progenitor: nearly 360° in the case of IC 4499, more than a complete wrap for Rup 106, and their apparent positioning as neighbours along a single great circle is coincidental.

Using the methodology of van den Bergh (1993) to classify the orbital parameters of IC 4499, the cluster is likely to be in a prograde orbit that is of a “plunging” type. However, the cluster lies near the limit for circular orbits, suggesting that there is a relatively high likelihood that it is on a mildly eccentric orbit. Placing the cluster in context, it appears quite normal for its galactocentric distance and metallicity, and membership in a tidal stream is not needed to explain its radial velocity. Because the predicted radial velocity of the Monoceros tidal stream is consistent with the expectations for the general field, further information is necessary before IC 4499 can definitely be assigned membership in a stream, or be inferred to have been accreted into the halo from a dwarf galaxy. Two observables that could help discriminate between models are the cluster proper motion and the detailed abundance ratios of the member stars.

The Monoceros stream model that matches the position and distance of IC 4499 predicts a range of proper motions in galactic coordinates, $(-4, -1) \lesssim (\mu_l, \mu_b) \lesssim (-2, +2) \text{ mas/yr}$. On the other hand, the Besançon model suggests that most late-type halo stars at IC 4499's location will have proper motions of $(\mu_l, \mu_b) \approx (-5 \pm 5, 0 \pm 5) \text{ mas/yr}$. From this it can be seen that a proper motion in the appropriate range for stream membership is not sufficient to ensure membership, since halo stars overlap in both components (although less so in μ_l). Proper motions could make a strong negative test in that the cluster could be excluded from stream membership via this measurement.

Detailed abundance ratios are a stronger test, because of the consistency of elemental abundance ratios among field and cluster halo stars (e.g., Fulbright, 2000, 2002) and the strong anomalies seen in dwarf spheroidal galaxy field stars (e.g., Shetrone et al., 2003; McWilliam & Smecker-Hane, 2005; Chou et al., 2010) and clusters (e.g., Bellazzini et al., 2008; Carretta et al., 2010, and references therein). In particular the $[\alpha/\text{Fe}]$ vs. $[\text{Fe}/\text{H}]$ trend and ratios of *s*- and *r*-process elements can give strong clues to the past star-formation history, initial mass function sampling, and loss of metals from a stellar system (Tolstoy et al., 2003; Venn et al., 2004). Because IC 4499 is not a very massive cluster, it is expected to be chemically homogeneous, and

high-resolution spectra of just a few stars should suffice to begin characterisation of its nucleosynthetic history.

4 CONCLUSIONS

We obtained near-infrared spectra of 636 red giants in and around the RR Lyrae-rich, extreme-southern globular cluster IC 4499. From spectra including the calcium triplet, we measured radial velocities by cross-correlation with template stars in well-studied globular clusters M68, M22, and M4. By combining the CaT equivalent widths with 2MASS K_s magnitudes we derived metallicities on the Carretta & Gratton (1997) scale following the methodology of Warren & Cole (2009). The relationship in our data between CaT equivalent widths, K_s , and $[\text{Fe}/\text{H}]$ is in good agreement with the work of Warren & Cole (2009). Our velocity and metallicity results for the comparison clusters agree well with literature values. 43 stars were found to be probable cluster members based on radial velocity association, culled by metallicity to alleviate the strong foreground contamination.

The heliocentric radial velocity of IC 4499 is $v_r = 31.5 \pm 0.4$ km/s. The velocity is typical of halo objects along this sightline, and also does not rule out membership in a tidal stream as proposed by Peñarrubia et al. (2005). The most powerful tests of stream membership, proper motion and detailed elemental abundance ratios, are not yet available for this cluster. Like many proposed associations (e.g., Piatti & Clariá, 2008) the status of IC 4499 is undecided.

The metallicity of IC 4499 is $[\text{Fe}/\text{H}] = -1.52 \pm 0.12$ on the scale of Carretta & Gratton (1997), which translates to -1.74 ± 0.10 on the Zinn & West (1984) scale. This agrees with photometric estimates from the cluster CMD and unpublished work by R. Cannon (1992), but disagrees with the earlier studies of RR Lyrae stars (Smith & Perkins, 1982). To the extent that studies of the relative ages of globular clusters (e.g., Salaris & Weiss, 2002) and of the Oosterhoof RR Lyrae period-metallicity relation (e.g., Sandage, 1993) incorrectly relied on overestimates of the cluster metallicity, the role of IC 4499 in these studies should be reassessed. If age is the dominant contributor to the second-parameter effect (Lee, 1992), then the evidence for a young age (Ferraro et al., 1995) for IC 4499 is weak, based on its intermediate HB type. The cluster is slightly metal-poor compared to most OoI clusters.

We follow the approach of Lane et al. (2009, 2010) to search for evidence of rotation in IC 4499. We confirm their results in M22 and M4, although the signal is noisy because we have measured less than half the number of stars. We are unable to detect evidence for rotation in IC 4499, which puts an upper limit of ≈ 1 km/s on the net cluster rotation.

We model the velocity dispersion of the cluster using a Plummer potential, finding the best-fit cluster parameters using a Markov Chain Monte Carlo simulation. The most likely central velocity dispersion is $\sigma_0 = 2.5 \pm 0.5$ km/s. Using the Plummer model this translates to a cluster dynamical mass of $93 \pm 37 \times 10^3 M_\odot$. This is in agreement with fits to the light profile by McLaughlin & van der Marel (2005), and using their photometry implies a mass-to-light ratio $M/L_V = 1.3$ in solar units; this result is quite normal for a globular cluster (e.g., Trager et al., 1993; Lane et al., 2010) and

says that no dark matter component is needed to explain the cluster dynamics.

ACKNOWLEDGMENTS

Travel support for AAC was provided by the Anglo-Australian Observatory (AAO). The AAO is funded by the British and Australian governments. WJH acknowledges the support of the Grote Reber Foundation. AAC would like to thank AAT support astronomer Paul Dobbie and night assistant Winston Campbell for their assistance during the observing run. This publication makes use of data products from the Two Micron All Sky Survey, which is a joint project of the University of Massachusetts and IPAC/Caltech, funded by NASA and the NSF. This research has made use of the WEBDA database, operated at the Institute for Astronomy of the University of Vienna. IRAF is distributed by the National Optical Astronomy Observatories. The European Organisation for Astronomical Research in the Southern Hemisphere (ESO) maintain and distribute SKYCAT. Thanks to Dr. Simon Wotherspoon of the University of Tasmania for scripting the MCMC algorithm.

REFERENCES

- Armandroff T. E., Da Costa G. S., 1986, *AJ*, 92, 777
- Armandroff T. E., Da Costa G. S., 1991, *AJ*, 101, 1329
- Armandroff T. E., Zinn R., 1988, *AJ*, 96, 92
- Battaglia G., Irwin M., Tolstoy E., Hill V., Helmi A., Letarte B., Jablonka P., 2008, *MNRAS*, 383, 183
- Bellazzini M., Ibata R. A., Chapman S. C., Mackey A. D., Monaco L., Irwin M. J., Martin N. F., Lewis G. F., Dallessandro E., 2008, *AJ*, 136, 1147
- Carollo D., Beers T. C., Lee Y. S., Chiba M., Norris J. E., Wilhelm R., Sivarani T., Marsteller B., Munn J. A., Bailer-Jones C. A. L., Fiorentin P. R., York D. G., 2007, *Nature*, 450, 1020
- Carretta E., Bragaglia A., Gratton R. G., Lucatello S., Bellazzini M., Catanzaro G., Leone F., Momany Y., Piotto G., D’Orazi V., 2010, *ArXiv e-prints*
- Carretta E., Gratton R. G., 1997, *A&AS*, 121, 95
- Chou M., Cunha K., Majewski S. R., Smith V. V., Patterson R. J., Martínez-Delgado D., Geisler D., 2010, *ApJ*, 708, 1290
- Clement C. M., Muzzin A., Dufton Q., Ponnampalam T., Wang J., Burford J., Richardson A., Rosebery T., Rowe J., Hogg H. S., 2001, *AJ*, 122, 2587
- Clement C. M., Rowe J., 2000, *AJ*, 120, 2579
- Cole A. A., Smecker-Hane T. A., Tolstoy E., Bosler T. L., Gallagher J. S., 2004, *MNRAS*, 347, 367
- Da Costa G. S., Held E. V., Saviane I., Gullieuszik M., 2009, *ApJ*, 705, 1481
- Dall’Ora M., Bono G., Storm J., Caputo F., Andreuzzi G., Marconi G., Monelli M., Ripepi V., Stetson P. B., Testa V., 2006, *Memorie della Societa Astronomica Italiana*, 77, 214
- Ferraro F. R., Montegriffo P., Origlia L., Fusi Pecci F., 2000, *AJ*, 119, 1282
- Ferraro I., Ferraro F. R., Pecci F. F., Corsi C. E., Buonanno R., 1995, *MNRAS*, 275, 1057

- Forbes D. A., Bridges T., 2010, MNRAS, 404, 1203
- Fourcade C. R., Laborde J. R., Arias J. C., 1974, A&AS, 18, 3
- Frinchaboy P. M., Majewski S. R., Crane J. D., Reid I. N., Rocha-Pinto H. J., Phelps R. L., Patterson R. J., Muñoz R. R., 2004, ApJL, 602, L21
- Frogel J. A., Cohen J. G., Persson S. E., 1983, ApJ, 275, 773
- Fulbright J. P., 2000, AJ, 120, 1841
- Fulbright J. P., 2002, AJ, 123, 404
- Fusi Pecci F., Bellazzini M., Cacciari C., Ferraro F. R., 1995, AJ, 110, 1664
- García-Vargas M. L., Molla M., Bressan A., 1998, A&AS, 130, 513
- Geisler D., Piatti A. E., Claria J. J., Minniti D., 1995, AJ, 109, 605
- Gilks W. R., Richardson S., Spiegelhalter D. J., 1998, Markov Chain Monte Carlo in Practice. Chapman and Hall, Boca Raton, Florida
- Grocholski A. J., Cole A. A., Sarajedini A., Geisler D., Smith V. V., 2006, AJ, 132, 1630
- Harris W. E., 1975, ApJS, 29, 397
- Harris W. E., 1996, VizieR Online Data Catalog, 7195, 0
- Helmi A., Navarro J. F., Meza A., Steinmetz M., Eke V. R., 2003, ApJL, 592, L25
- Ibata R. A., Irwin M. J., Lewis G. F., Ferguson A. M. N., Tanvir N., 2003, MNRAS, 340, L21
- Kaluzny J., Thompson I. B., 2001, VizieR Online Data Catalog, 337, 30899
- King I. R., 1966, AJ, 71, 64
- Kraft R. P., Ivans I. I., 2003, PASP, 115, 143
- Lane R. R., Kiss L. L., Lewis G. F., Ibata R. A., Siebert A., Bedding T. R., Székely P., 2009, MNRAS, 400, 917
- Lane R. R., Kiss L. L., Lewis G. F., Ibata R. A., Siebert A., Bedding T. R., Székely P., Balog Z., Szabó G. M., 2010, MNRAS, pp 799–+
- Lee J., Carney B. W., 1999, AJ, 118, 1373
- Lee Y., 1989, PhD thesis, Yale Univ., New Haven, CT.
- Lee Y., 1992, PASP, 104, 798
- Lee Y., Demarque P., Zinn R., 1990, ApJ, 350, 155
- Liu T., Janes K. A., 1990, ApJ, 360, 561
- Longmore A. J., Dixon R., Skillen I., Jameson R. F., Fernley J. A., 1990, MNRAS, 247, 684
- Mackey A. D., Gilmore G. F., 2003, MNRAS, 345, 747
- Martin N. F., Ibata R. A., Bellazzini M., Irwin M. J., Lewis G. F., Dehnen W., 2004, MNRAS, 348, 12
- Martin N. F., Ibata R. A., Conn B. C., Lewis G. F., Bellazzini M., Irwin M. J., 2005, MNRAS, 362, 906
- McLaughlin D. E., van der Marel R. P., 2005, ApJS, 161, 304
- McWilliam A., Smecker-Hane T. A., 2005, ApJL, 622, L29
- Morrison H. L., Mateo M., Olszewski E. W., Harding P., Dohm-Palmer R. C., Freeman K. C., Norris J. E., Morita M., 2000, AJ, 119, 2254
- Newberg H. J., Yanny B., Rockosi C., Grebel E. K., Rix H., Brinkmann J., Csabai I., Hennessy G., Hindsley R. B., Ibata R., Ivezić Z., Lamb D., Nash E. T., Odenkirchen M., Rave H. A., Schneider D. P., Smith J. A., Stolte A., York D. G., 2002, ApJ, 569, 245
- Peñarrubia J., Martínez-Delgado D., Rix H. W., Gómez-Flechoso M. A., Munn J., Newberg H., Bell E. F., Yanny B., Zucker D., Grebel E. K., 2005, ApJ, 626, 128
- Peterson R. C., Cudworth K. M., 1994, ApJ, 420, 612
- Peterson R. C., Rees R. F., Cudworth K. M., 1995, ApJ, 443, 124
- Piatti A. E., Clariá J. J., 2008, MNRAS, 390, L54
- Pickering E. C., 1908, Annals of Harvard College Observatory, 60, 147
- Plummer H. C., 1911, MNRAS, 71, 460
- Pritzl B., Smith H. A., Catelan M., Sweigart A. V., 2000, ApJL, 530, L41
- Robin A. C., Reylé C., Derrière S., Picaud S., 2003, A&A, 409, 523
- Rutledge G. A., Hesser J. E., Stetson P. B., 1997, PASP, 109, 907
- Salaris M., Weiss A., 2002, A&A, 388, 492
- Sandage A., 1993, AJ, 106, 687
- Sarajedini A., 1993, AJ, 105, 2172
- Sharp R., Saunders W., Smith G., Churilov V., Correll D., Dawson J., Farrel T., Frost G., Haynes R., Heald R., Lankshear A., Mayfield D., Waller L., Whittard D., 2006, in Society of Photo-Optical Instrumentation Engineers (SPIE) Conference Series Vol. 6269 of Society of Photo-Optical Instrumentation Engineers (SPIE) Conference Series, Performance of AAOmega: the AAT multi-purpose fiber-fed spectrograph
- Shetrone M., Venn K. A., Tolstoy E., Primas F., Hill V., Kaufer A., 2003, AJ, 125, 684
- Skrutskie M. F. e. a., 2006, AJ, 131, 1163
- Smith G., Drake J. J., 1990, A&A, 231, 125
- Smith H. A., 1984, PASP, 96, 505
- Smith H. A., Perkins G. J., 1982, ApJ, 261, 576
- Storm J., 2004, A&A, 415, 987
- Tolstoy E., Venn K. A., Shetrone M., Primas F., Hill V., Kaufer A., Szeifert T., 2003, AJ, 125, 707
- Tonry J., Davis M., 1979, AJ, 84, 1511
- Trager S. C., Djorgovski S., King I. R., 1993, in S. G. Djorgovski & G. Meylan ed., Structure and Dynamics of Globular Clusters Vol. 50 of Astronomical Society of the Pacific Conference Series, Structural Parameters of Galactic Globular Clusters. pp 347–+
- van den Bergh S., 1993, AJ, 105, 971
- Venn K. A., Irwin M., Shetrone M. D., Tout C. A., Hill V., Tolstoy E., 2004, AJ, 128, 1177
- Vivas A. K. e. a., 2001, ApJL, 554, L33
- Walker A. R., Nemeč J. M., 1996, AJ, 112, 2026
- Warren S. R., Cole A. A., 2009, MNRAS, 393, 272
- Yanny B. e. a., 2000, ApJ, 540, 825
- Younger J. D., Besla G., Cox T. J., Hernquist L., Robertson B., Willman B., 2008, ApJL, 676, L21
- Zinn R., West M. J., 1984, ApJS, 55, 45

Table 1. Log of Observations

Target	α (J2000) ^a	δ (J2000) ^a	UT start	Airmass	Seeing (")	t_{exp} (s)	[Fe/H] (dex) ^b	V_r (km/s)
M68	12 39 28	-25 15 39	11:43:55	1.06	1.4	2×360	-1.99 ±0.06	-96.4 ±3.9 ^c
M4	16 23 34	-26 32 01	18:16:28	1.72	1.4	2×180	-1.19 ±0.03	70.9 ±0.6 ^d
M22	18 36 25	-23 54 16	19:14:59	1.32	1.4	2×180	-1.48 ±0.03 [†]	-148.8 ±0.8 ^e
IC 4499 1	15 00 21	-82 12 46	13:09:58	1.60	1.4	2×1800		
IC 4499 2	15 00 22	-82 12 52	15:34:27	1.67	1.4	2×1800		

^aCentre of AAOmega/2dF field; ^bCarretta & Gratton (1997); ^cGeisler et al. (1995); ^dPeterson et al. (1995); ^ePeterson & Cudworth (1994). [†]A significant range is present (Da Costa et al., 2009).

Table 2. Summary of results.

Cluster	N_*	W' (Å)	K_{HB} (mag)	[Fe/H]	Δ [Fe/H]	V_r (km/s)	ΔV_r (km/s)
M68	51	2.59 ±0.35	14.4 ^a	-1.88 ±0.13	0.11 ±0.14	-98.6 ±1.5	-4.2 ±4.2
M4	70	4.90 ±0.34	11.13	-1.12 ±0.14	0.07 ±0.14	65.7 ±0.9	5.2 ±1.1
M22	81	3.61 ±0.46	12.21	-1.55 ±0.17	-0.07 ±0.17	-150.5 ±1.3	-1.7 ±1.5
IC 4499	43	3.70 ±0.29	15.97	-1.52 ±0.12		31.5 ±0.4	

^aDall’Ora et al. (2006). Δ Difference, measured–literature value.

Table 3. IC 4499 Members.

ID	α (J2000) ^a	δ (J2000) ^a	V_r (km/s)	ΣW (Å)	K_S^a (mag)
4976	14:59:33.41	-82:09:17.80	31.40±1.49	5.51±0.36	12.55
4983	15:01:05.98	-82:12:36.93	31.21±1.49	5.00±0.52	12.65
5034	14:58:38.62	-82:10:30.86	32.42±1.46	4.27±0.66	14.22
5420	15:00:42.16	-82:08:32.40	32.88±1.93	4.73±0.90	13.98
5437	15:01:49.80	-82:13:39.74	31.16±1.48	5.06±0.94	14.47
5447	14:59:01.37	-82:10:50.80	28.91±1.96	5.07±0.70	13.57
5478	14:58:54.40	-82:16:34.04	33.44±1.46	4.58±0.56	13.79
5488	15:02:14.17	-82:15:35.02	30.88±1.49	4.95±1.33	14.70
5595	14:59:46.75	-82:16:15.61	30.47±1.49	5.64±0.46	12.31
5644	14:59:40.00	-82:12:22.84	27.48±1.48	4.77±0.68	13.89
5649	14:58:19.16	-82:08:30.86	30.89±1.66	6.03±0.45	11.61
5914	14:58:56.49	-82:13:14.09	32.28±1.46	3.80±0.81	14.22
5916	14:58:54.78	-82:03:44.48	31.29±1.67	5.72±0.49	12.16
5971	15:00:38.30	-82:11:12.03	30.18±1.40	6.60±0.49	10.77
6150	14:59:50.74	-82:13:10.60	30.86±1.49	4.32±0.61	13.81
6210	14:59:18.66	-82:12:40.50	30.62±1.93	5.45±0.46	12.64
6266	15:00:05.66	-82:15:51.72	34.06±1.65	4.24±1.01	14.78
6302	15:00:10.58	-82:11:17.03	31.88±1.50	5.70±0.40	12.22
6370	14:57:18.38	-82:10:41.52	31.84±1.48	4.43±0.84	14.51
6389	15:01:25.51	-82:20:14.43	30.99±1.49	5.61±0.27	11.99
6450	15:01:55.59	-82:10:45.69	34.28±1.49	5.10±0.47	12.59
6478	14:59:45.22	-82:14:47.23	29.58±1.47	4.88±0.57	13.76
6688	15:04:56.01	-82:20:08.58	33.09±1.63	5.19±1.45	14.79
6689	15:01:21.54	-82:13:45.49	31.71±1.30	4.56±0.91	14.41
6693	15:01:31.47	-82:12:24.68	29.63±1.44	3.93±0.91	14.49
6698	15:00:17.12	-82:16:35.09	29.65±1.48	5.00±0.37	13.10
6703	15:00:34.26	-82:14:45.50	38.08±1.49	5.52±0.40	11.35
6710	14:59:47.84	-82:14:13.06	36.36±1.39	4.02±1.08	14.75
6718	15:00:06.81	-82:11:52.33	26.83±1.48	4.54±0.62	13.93
6732	15:01:05.76	-82:12:57.37	28.30±1.50	4.82±0.69	13.79
6847	15:00:51.51	-82:12:50.99	34.76±1.58	4.07±1.39	14.97
6850	15:02:54.39	-82:11:43.51	31.56±1.93	5.42±0.50	12.93
7024	14:58:40.81	-82:10:36.05	31.65±1.50	4.01±1.14	14.09
7088	14:59:55.26	-82:13:13.16	29.35±1.46	4.68±0.82	14.65
7089	15:00:58.89	-82:14:09.08	30.09±1.94	4.58±0.52	13.64
7126	14:58:59.03	-82:08:33.25	29.97±1.92	4.84±0.60	13.49
7162	15:00:47.33	-82:12:51.62	35.64±1.51	4.38±0.93	14.06
7290	15:00:39.11	-82:13:17.03	25.95±1.48	4.83±0.73	14.11
7508	14:59:42.17	-82:10:05.79	31.96±2.00	4.72±2.02	14.16
7529	15:00:17.01	-82:11:11.46	31.52±1.71	5.79±0.41	11.94
7558	14:57:40.75	-82:10:33.69	30.41±1.49	5.77±1.03	11.58
7575	14:59:40.44	-82:16:04.08	31.52±1.48	5.98±0.33	11.78
7910	14:59:47.29	-82:11:09.15	33.05±1.50	4.68±0.56	14.06

^aFrom 2MASS point source catalogue.